

UC Davis

UC Davis Previously Published Works

Title

Assessment of Multifocal Electroretinogram Abnormalities and Their Relation to Morphologic Characteristics in Patients With Large Drusen

Permalink

<https://escholarship.org/uc/item/6qr0b842>

Journal

JAMA Ophthalmology, 121(10)

ISSN

2168-6165

Authors

Gerth, Christina
Hauser, David
Delahunt, Peter B
[et al.](#)

Publication Date

2003-10-01

DOI

10.1001/archopht.121.10.1404

Peer reviewed

Assessment of Multifocal Electroretinogram Abnormalities and Their Relation to Morphologic Characteristics in Patients With Large Drusen

Christina Gerth, MD; David Hauser, MD; Peter B. Delahunt, PhD; Lawrence S. Morse, MD, PhD; John S. Werner, PhD

Objectives: To determine the extent of functional changes in the first-order kernel multifocal electroretinogram (mfERG) responses in patients with large drusen by means of a localized analysis and to determine correlations between mfERG responses and morphologic changes.

Methods: Thirty-one eyes from 20 patients ages 58 to 84 years with large drusen (≥ 5 drusen ≥ 63 μm diameter) were studied. The mfERGs were recorded with a stimulus of 103 hexagons and a flash intensity of 2.67 candela (cd) $\cdot\text{s}^{-1}\cdot\text{m}^{-2}$. Each of the 103 single first-order kernel mfERG responses was analyzed and compared with those of age-matched healthy control subjects. Imaging studies, including color stereo fundus photography, red-free fundus photography, and fluorescein angiography, were performed in all patients, and morphologic changes (drusen in red-free fundus photography, staining or window defect in fluorescein angiography) were determined with a digital measurement tool.

The mfERG responses were correlated to areas with and without morphologic changes.

Results: Reduced responses were found in 10.0% (scalar products) and 4.0% (response densities) and delayed implicit times in 13.8% (N1), 18.9% (P1), and 23.8% (N2) of all mfERGs. Abnormal mfERG responses extended up to 25° in radius. Significant morphologic-functional relations were detected in only a few patients. Abnormal mfERG variables were present in areas without morphologic changes.

Conclusions: Patients with large drusen exhibit functional changes in the cone-driven pathways evaluated by the mfERG, indexed particularly by implicit times. Morphologically visible changes do not predict retinal function. Large drusen are associated with a more general retinal dysfunction.

Arch Ophthalmol. 2003;121:1404-1414

From the Department of Ophthalmology and Section of Neurobiology, Physiology, and Behavior, University of California, Davis. Dr Gerth is now with the Department of Ophthalmology, St Franziskus-Hospital, Münster, Germany. The authors have no relevant financial interest in this article.

LARGE DRUSEN are a characteristic sign of age-related macular degeneration (AMD) and are strongly predictive of late-stage AMD.¹⁻³

The pathogenesis is not yet known, although several risk factors such as cardiovascular disease and smoking have been identified.^{1,4,5} Drusen are deposits of extracellular debris containing neutral fats, phospholipids,⁶ and other cellular and extracellular components⁷ and are derived from photoreceptor outer segments.⁸ They are localized between the basement membrane of the retinal pigment epithelial cells and the inner collagenous zone of Bruch's membrane. A thickened Bruch's membrane and retinal pigment epithelium and photoreceptor atrophy are found directly over drusen.^{9,10} With increasing deposits, there is disruption of functional circuits that include photoreceptors, retinal pigment epithelium, Bruch's membrane, and choriocapillaris. Retinal pigment epithelium derangement leads to photore-

ceptor death.⁸ Histologic studies have demonstrated that foveal cones (central 2.8°) are resistant to degeneration, but the parafoveal photoreceptors are degenerated in the nonexudative form of AMD.^{9,10}

In the present study, we tested the hypothesis that large drusen (≥ 63 μm) are correlated with retinal dysfunction under photopic conditions and examined whether large drusen point to specific sites of retinal dysfunction or to more generally affected areas. A localized functional assessment was made possible by the multifocal electroretinogram (mfERG) technique developed by Sutter and Tran.^{11,12} Previous mfERG studies in patients with drusen showed conflicting results,¹³⁻¹⁵ included only a small number of patients with AMD, or did not compare patients with drusen individually with control data.¹⁶⁻¹⁸ Furthermore, all but the study by Martinsen¹⁹ averaged mfERG responses and therefore lost the topographic information about retinal function. To achieve a localized evaluation of the

Table 1. Visual Acuity of the 20 Patients With Large Drusen

Patient No./ Sex/Age, y	Eye	Visual Acuity
1/F/68	OD	20/20
2/F/75	OS	20/50
3/F/77	OD	20/40
3/F/77	OS	20/32
4/F/81	OD	20/50
	OS	20/50
5/F/73	OD	20/20
	OS	20/16
6/F/74	OD	20/20
	OS	20/16
7/M/68	OD	20/20
8/F/67	OD	20/20
9/F/74	OD	20/16
10/F/69	OS	20/25
11/M/79	OS	20/32
12/F/83	OS	20/32
13/F/71	OD	20/25
	OS	20/20
14/M/84	OD	20/25
	OS	20/40
15/F/70	OD	20/25
	OS	20/25
16/F/58	OD	20/20
17/M/69	OD	20/40
	OS	20/32
18/F/76	OD	20/32
	OS	20/32
19/F/74	OD	20/25
	OS	20/20
20/M/76	OD	20/50
	OS	20/40

cone-driven pathways and to correlate it with fundus morphologic characteristics, we analyzed each of the single mfERG responses without spatial averaging. We selected patients on the basis of their drusen morphologic characteristics and measured the area of drusen by means of imaging by color stereo and red-free fundus photography (RF) and fluorescein angiography (FA). We found significant localized retinal dysfunction, but it was not significantly related to the morphologically visible changes in most eyes. Significantly abnormal mfERG responses were not restricted to areas with drusen. Implicit times were more sensitive in demonstrating retinal abnormalities than response density.

METHODS

PATIENTS

Twenty patients, 5 men and 15 women, with large drusen were tested. Their ages ranged from 58 to 84 years (mean \pm SD, 74 ± 6 years). Retinal inclusion criteria were 5 or more drusen at least 63 μ m diameter within 2250 μ m from the foveal center. Eyes with signs of neovascular maculopathy, geographic atrophy, optic nerve head findings, or previous retinal surgery were excluded. Patients with diabetes mellitus, neurologic disorders, or medication known to disrupt visual function were not included. Thirty-one eyes were tested. Eleven patients were tested binocularly and 9 patients monocularly. All subjects demonstrated a best-corrected visual acuity of 20/50 or better (Early

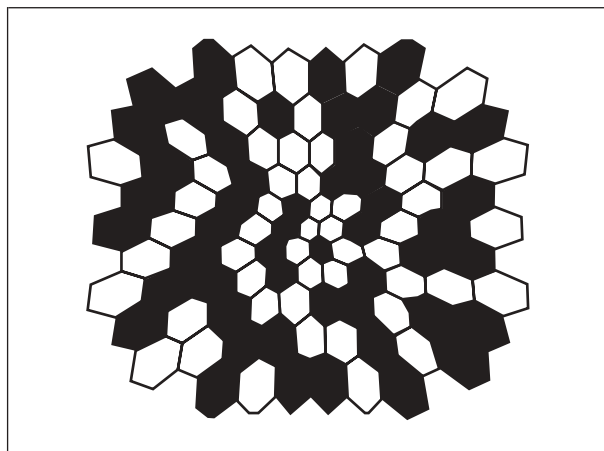


Figure 1. Stimulus pattern consisting of 103 scaled hexagons. Each of the hexagons flashed pseudorandomly with a flash intensity of 2.67 candela ($\text{cd} \cdot \text{s}^{-1} \cdot \text{m}^{-2}$).

Treatment Diabetic Retinopathy Study charts) in the tested eye (**Table 1**). Among the 31 eyes tested, 7 were pseudophakic. Intraocular pressure was 22 mm Hg or less in all eyes tested.

CONTROL GROUP

Carefully screened healthy subjects were used as data controls (10 subjects ages 50-59 years and 60-69 years, and 9 subjects ages 70-80 years).²⁰ Data from pseudophakic patients (mean \pm SD age, 77 ± 3 years) were compared with data from a healthy pseudophakic control group of 9 subjects (mean \pm SD age, 72 ± 4 years). The retinas of all control subjects were found to have no more than 5 small ($< 63 \mu\text{m}$) drusen and no vascular, retinal, choroidal, or optic nerve findings known to disrupt visual function. All control subjects demonstrated a corrected Snellen acuity of 20/20 or better in the tested eye, as well as normal color vision when tested with an anomaloscope (Neitz Instrument Co, Tokyo, Japan), pseudoisochromatic plates (AO H-R-R; American Optical Co, Buffalo, NY), and the Farnsworth F-2 plate (Naval Submarine Medical Research Laboratory, Groton, Conn).

Written informed consent was obtained from both patients and controls in accordance with the Tenets of Helsinki, and with the approval of the Office of Human Research Protection of the University of California, Davis, School of Medicine.

MULTIFOCAL ERG PROCEDURE

The recordings were performed with a stimulus-refractor unit (frame rate, 75 Hz) (VERIS, version 4.3.; Electro-Diagnostic Imaging, Inc, San Mateo, Calif). The mfERGs were recorded on dilated pupils with a bipolar contact lens electrode (Burian-Allen; Hansen Ophthalmic Development Laboratory, Coralville, Iowa). Subjects were corrected for refractive errors by adjusting their own correction on the refractor unit to optimally focus the stimulus. Before and during recording, a correct and centered position of the contact lens in relation to the pupil and to the stimulus was ensured by monitoring a video camera image. All recordings were done by the same person (C.G.). The recordings were performed under room light conditions. Noise-contaminated segments were rejected and repeated.

The stimulus consisted of 103 scaled hexagons (**Figure 1**) flashed pseudorandomly at intervals of 13.3 milliseconds (m-sequence-length $2^{14} - 1$) on a dark background ($< 1 \text{ cd} \cdot \text{m}^{-2}$). The flash intensity was $2.67 \text{ cd} \cdot \text{s} \cdot \text{m}^{-2}$ ($200 \text{ cd} \cdot \text{m}^{-2}$ per 75 Hz). Signals were sampled at 1200 Hz (ie, 0.83 millisecond between samples). The data were acquired at a gain of 10^5 over a frequency range of 10 to 300 Hz (Grass preampli-

fier ICP 511; Grass Instruments, West Warwick, RI). A 4.8° black fixation cross was used. Stimulus luminance was calibrated with the autocalibrator (Electro-Diagnostic Imaging, Inc). The recording protocol was chosen according to the recommended guidelines of the International Society for Clinical Electrophysiology of Vision for basic mfERG.²¹

IMAGING PROCEDURES

Color stereo and RF fundus photography and FA were performed on a ×50 retinal camera (TRC; Topcon Corporation,

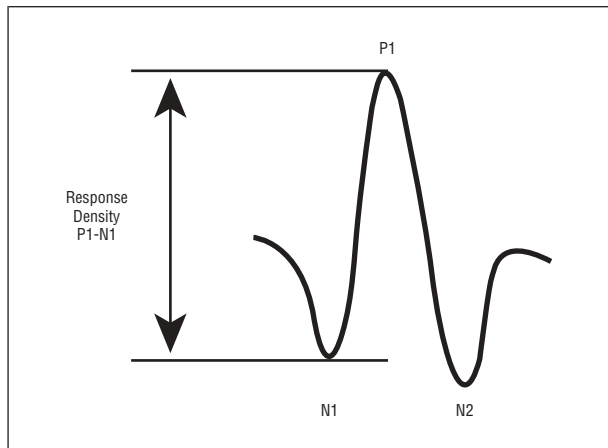


Figure 2. Response density P1-N1 and implicit times N1, P1, and N2, analyzed in each of the 103 multifocal electroretinograms.

Tokyo) for each patient. The RF and FA were recorded over the central field of 30°. In all but 2 patients, imaging procedures and mfERG recording were performed on the same day. In most cases, FA was performed after the mfERG test; if not, FA was finished at least 2 hours before the mfERG recording. For 2 patients, mfERG recording was performed 2 days after the imaging procedures.

DATA ANALYSIS

Multifocal ERGs

Each of the 103 areas of the mfERGs in patients and controls was analyzed separately. One iteration of an artifact rejection procedure but no spatial smoothing was applied to the raw data. Using VERIS 4.3., first-order kernel responses were evaluated for implicit times N1 (first negative trough), P1 (first positive peak), and N2 (second negative trough); amplitudes P1 to N1 (from the first negative trough to the first positive peak) (**Figure 2**); and the scalar products. Amplitudes were measured on the response density-scaled regional averages. Waveform parameters were exported from VERIS 4.3. to MATLAB (available at: <http://www.mathworks.com/>) for graphical and statistical analyses. The mfERG data were compared with data from age-matched controls separately for phakic and pseudophakic patients because the altered optical properties result in different response latencies and amplitudes.²² Response losses or delays of more than 2 SDs from normal are described as significantly abnormal.

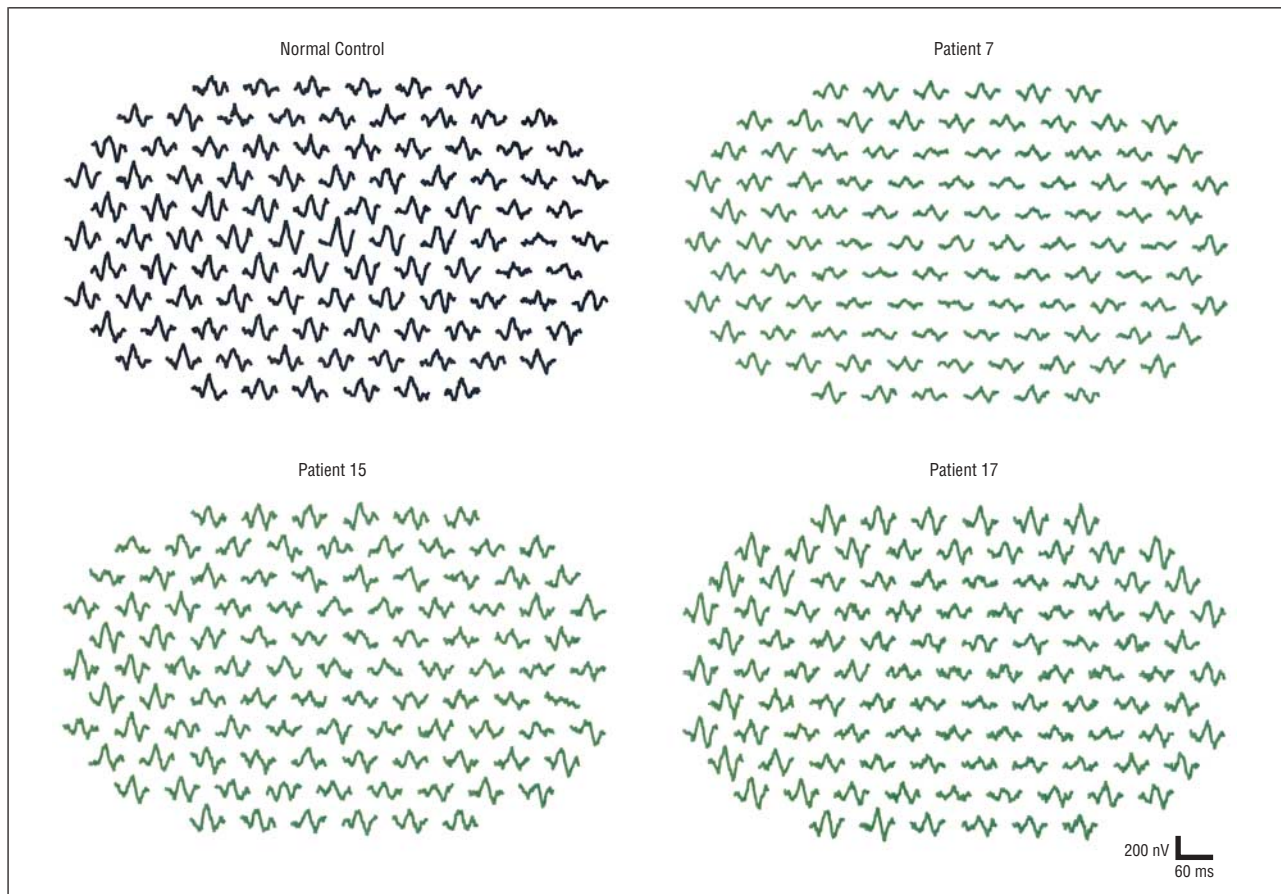


Figure 3. Multifocal electroretinogram traces from the right eyes of 1 typical control subject (age 77 years) (black traces, top left panel) and patients 7, 15, and 17 (green traces).

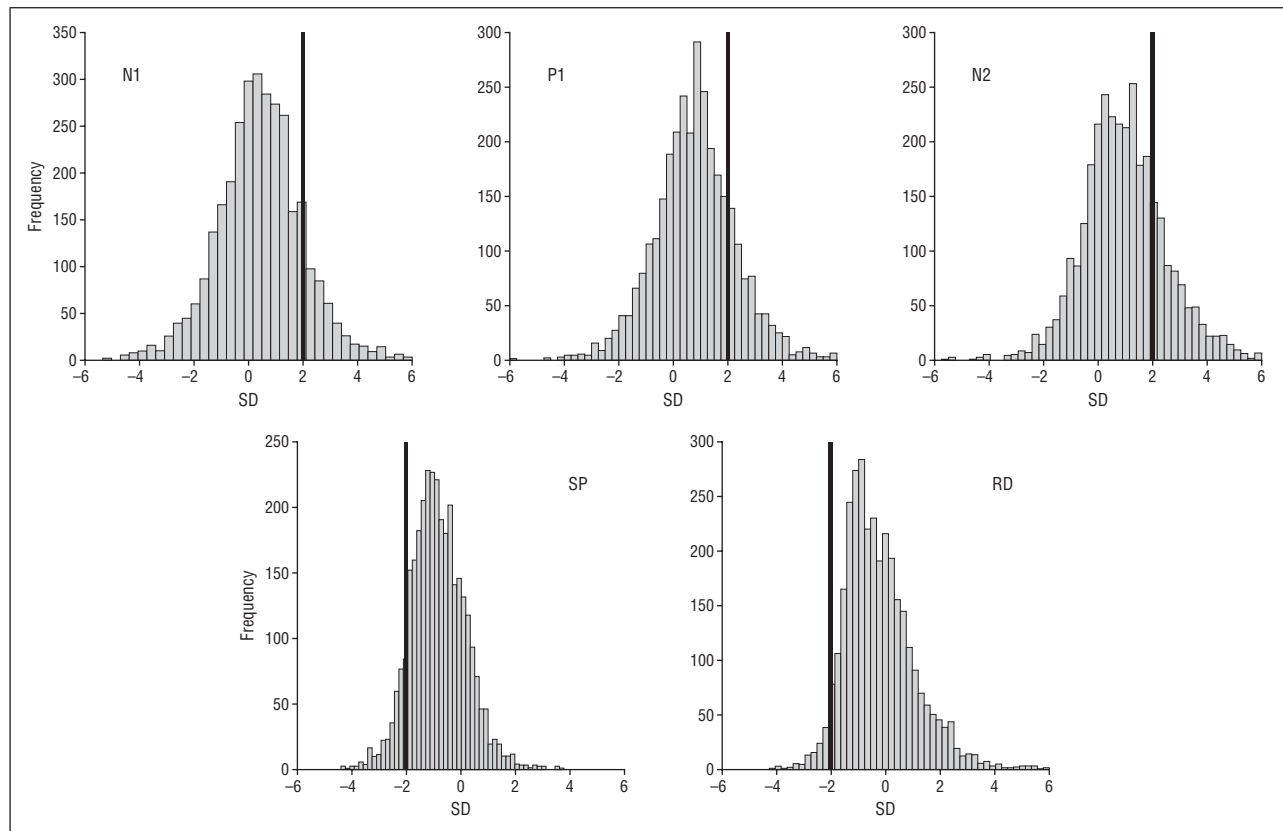


Figure 4. Comparison of all multifocal electroretinogram (mfERG) responses with the healthy control group in histograms for implicit times N1, P1, and N2 and for the scalar product (SP) and response density P1-N1 (RD). The components of the mfERG responses for each patient were converted to SD units from those of the control subjects. Numbers of mfERGs (y-axis) are plotted as a function of SDs from control normal data (x-axis). Bold line illustrates the point of significantly abnormal data (>2 SDs for implicit times, <2 SDs for scalar product and response density P1-N1).

Imaging

The RF and FA were analyzed for the same areas used in the mfERG. To accomplish this localized analysis, the scaled mfERG hexagons were superimposed on the RF or FA images. The central hexagon was centered at the foveal center. Correct alignment was ensured by the optic disc location with a distance of 15° to 18° from the foveal center. Areas of drusen or staining or window defect were digitally acquired from RF images on the basis of stereo fundus photography or late-stage FA images in each of the superimposed hexagons (WinStation 1400; Ophthalmic Imaging Systems, Sacramento, Calif). Morphologically changed areas are expressed as a percentage of the total measured area.

The analyzed variables of the mfERG responses for each patient were converted to SD units from our normative database. The relation between these units of deviation and the morphologic changes were tested by means of linear regression. (Scatter plots did not suggest any nonlinear relations.)

RESULTS

COMPARISON WITH AGE-MATCHED CONTROLS

Figure 3 shows first-order kernel trace arrays from 1 typical control subject and 3 patients. The normal mfERG is characterized by a large and pronounced central response and decreasing responses outward to the peripheral areas. In the patients' mfERG, such a peaked central response is missing. To investigate the localized responses, each of the 103 mfERGs was analyzed in terms

of the scalar product, response density, and implicit times N1, P1, and N2.

The data from all 3193 mfERGs (103 areas tested in 31 eyes) were compared with those from the age-matched controls. The results are illustrated in histograms in **Figure 4**. The upper row shows the comparison in implicit times N1, P1, and N2, while the lower row presents the results for scalar product (SP) and response density P1-N1 (RD). The data are plotted in SD units relative to the control data. Delayed implicit times and reduced scalar products or response densities of more than 2 SDs are marked with a bold line. Scalar products are sensitive to changes in wave shape¹¹ and can therefore reflect differences in implicit time and response density. Abnormal scalar products were found in 10.0% of all mfERGs. Implicit times were more sensitive than response density for detecting abnormal retinal responses; 4.0% of all mfERGs showed abnormal response densities compared with abnormal implicit times N1, P1, and N2 in 13.8%, 18.9%, and 23.8% of all mfERGs, respectively.

Does the response delay increase as the retinal response develops? In other words, do we find a significantly delayed implicit time N2 whenever responses show a delayed implicit time N1 or P1? To investigate this, mfERGs with significantly delayed implicit time N1 were analyzed separately for their implicit times P1 and N2. We found that 21.9% and 23.4% of those mfERGs showed significantly delayed implicit time P1 and N2, respectively.

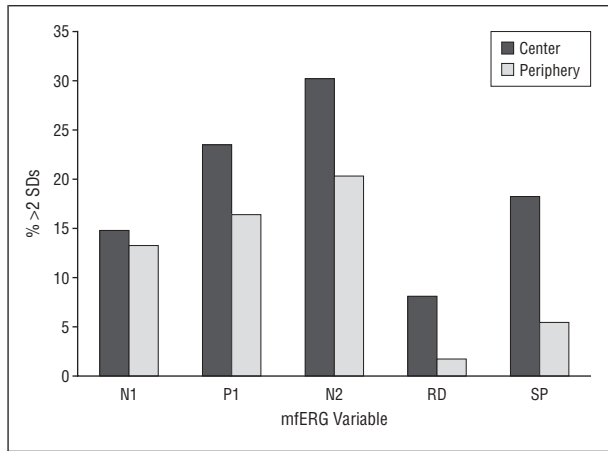


Figure 5. Multifocal electroretinograms (mfERGs) analyzed separately for the central 15° (center) and the areas outside of 15° (periphery). Percentages of abnormal mfERGs (>2 SDs for implicit times, <2 SDs for scalar product [SP] and response density P1-N1 [RD]) are plotted for implicit times N1, P1, N2; RD; and SP.

Table 2. Number of Eyes With Significant Correlations Between mfERG and Morphologic Changes*

mfERG Variable	Drusen Area	Staining/Window Defect Area
Scalar product	7	7
Response density P1-N1	2	4
Implicit time N1	2	2
Implicit time P1	1	2
Implicit time N2	3	7

Abbreviation: mfERG, multifocal electroretinogram.

*Drusen area measured in red-free fundus photography and staining/window defect area measured on fluorescein angiography. A total of 31 eyes were included (eg, 7 means that in 7 of 31 eyes tested, a significant correlation between the mfERG variable and the morphological change was found).

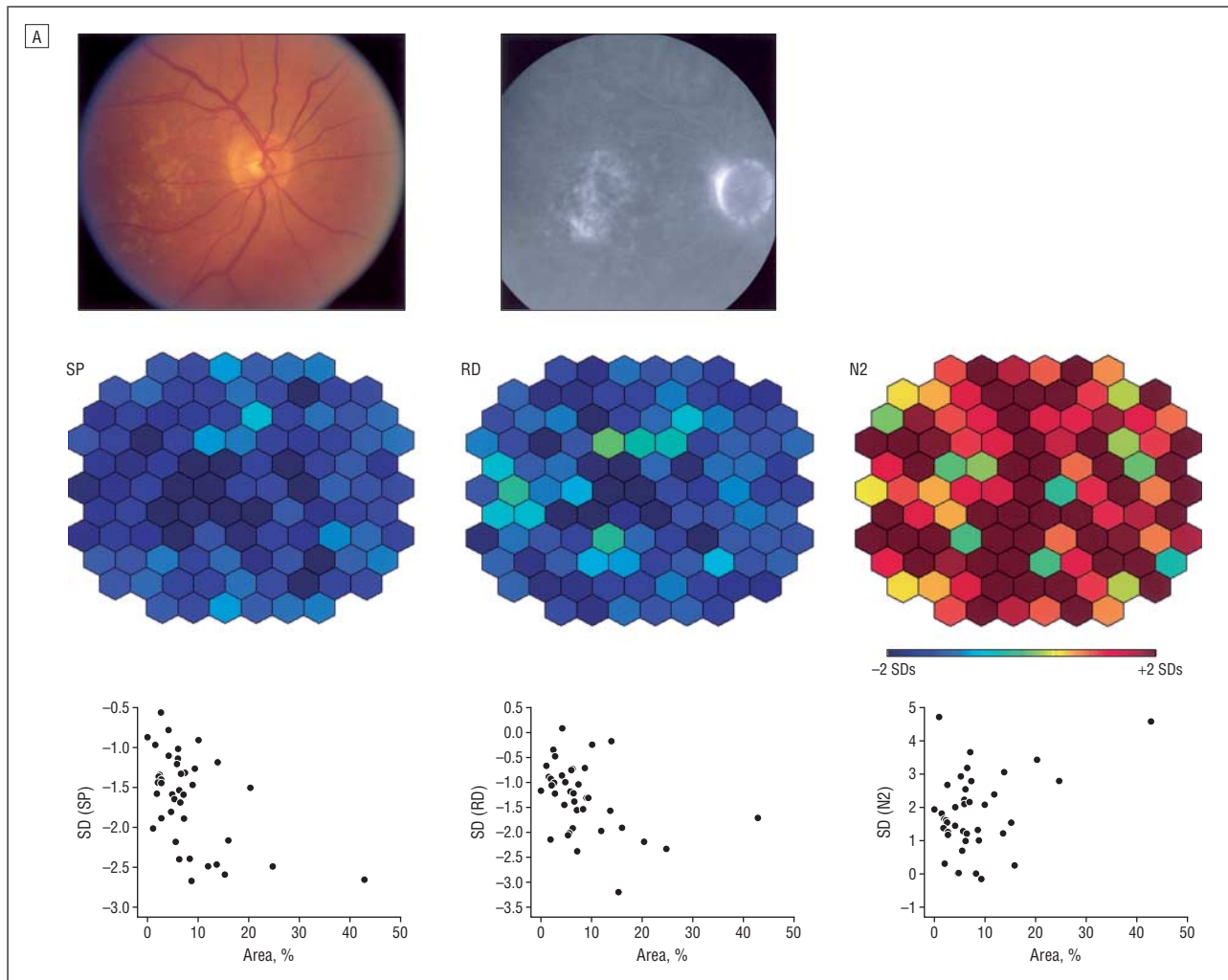


Figure 6A. Correlation of retinal dysfunction and morphologic characteristics for patient 3 (right eye). Color fundus photographs and fluorescein angiograms are shown to illustrate morphologic changes (top row). Multifocal electroretinogram (mfERG) variables are plotted in color-coded units of SD from the control subjects (scalar product [SP], response density P1-N1 [RD], and implicit time N2) (middle row). Abnormal scalar products and response densities are coded in dark blue (>2 SDs) and delayed implicit times of more than 2 SDs in red. Significant correlation between morphologic changes (staining or window defect area on fluorescein angiograms) and the same mfERG variables shown in the middle panel are demonstrated in scatter diagrams (bottom row). Plotted is the percentage of affected area (x-axis) as a function of scalar product or response density loss or implicit time delay (y-axis).

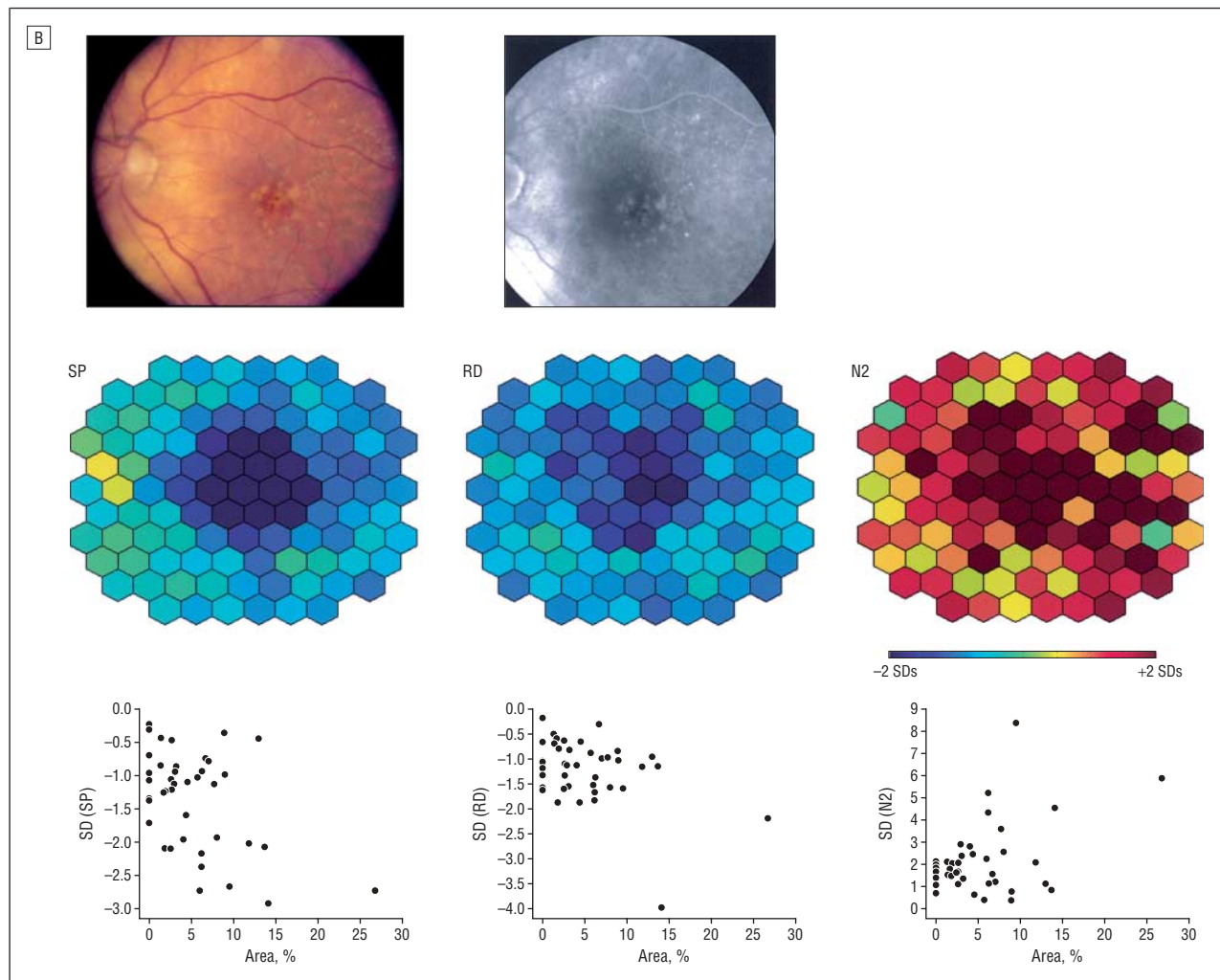


Figure 6B. Correlation of retinal dysfunction and morphologic characteristics for patient 4 (left eye). Color fundus photographs and fluorescein angiograms are shown to illustrate morphologic changes (top row). Multifocal electroretinogram (mfERG) variables are plotted in color-coded units of SD from the control subjects (scalar product [SP], response density P1-N1 [RD], and implicit time N2) (middle row). See the legend to Figure 6A for an explanation of the color coding and scatter diagrams.

Similar data resulted from the analysis of the mfERGs, with significantly delayed implicit time P1 and N2. The mfERGs with abnormal implicit time P1 showed delayed implicit times N1 and N2 in 30.0% and 37.8%, respectively. The mfERGs with significantly delayed N2 showed abnormal implicit time N1 and P1 in 40.4% and 47.6%, respectively. Retinal areas with delayed implicit times N1 or P1 did not invariably develop delayed implicit time N2.

TOPOGRAPHIC DISTRIBUTION OF ABNORMAL RESPONSES

To investigate the topographic distribution of abnormal responses, the analysis was repeated for the retinal areas within and outside of 15°. (Figure 5). The central 15° is more often affected by disease than the area outside 15°. Abnormal responses in the scalar product and the response density P1-N1 were found in 18.2% and 8.1% for the central area, compared with 5.4% and 1.7% for the area outside of 15°, respectively. Implicit times were more sensitive than response density or scalar product

in detecting abnormal responses in the areas outside of 15°. Significantly delayed implicit times N1, P1, and N2 were found in 13.2%, 16.3%, and 20.2% of the areas outside 15°, respectively.

RELATION BETWEEN FUNCTIONAL AND MORPHOLOGIC DATA

The relation between morphologic changes (drusen in RF or staining or window defect in FA) and the 5 analyzed mfERG variables were tested for each eye. As explained in the "Methods" section, the patients' RF and FA images were digitally analyzed for the same areas in which the mfERG was recorded. The pathological area (drusen in RF or staining or window defect in FA) was divided by the total area and expressed as a percentage. The analyzed variables of the mfERG responses for each patient (in SDs from those of the control subjects) were then correlated with the amount of morphologic change in all areas recorded by the imaging studies (central field of 30°).

As shown in Table 2, most eyes did not show a significant relation between morphologic features and reti-

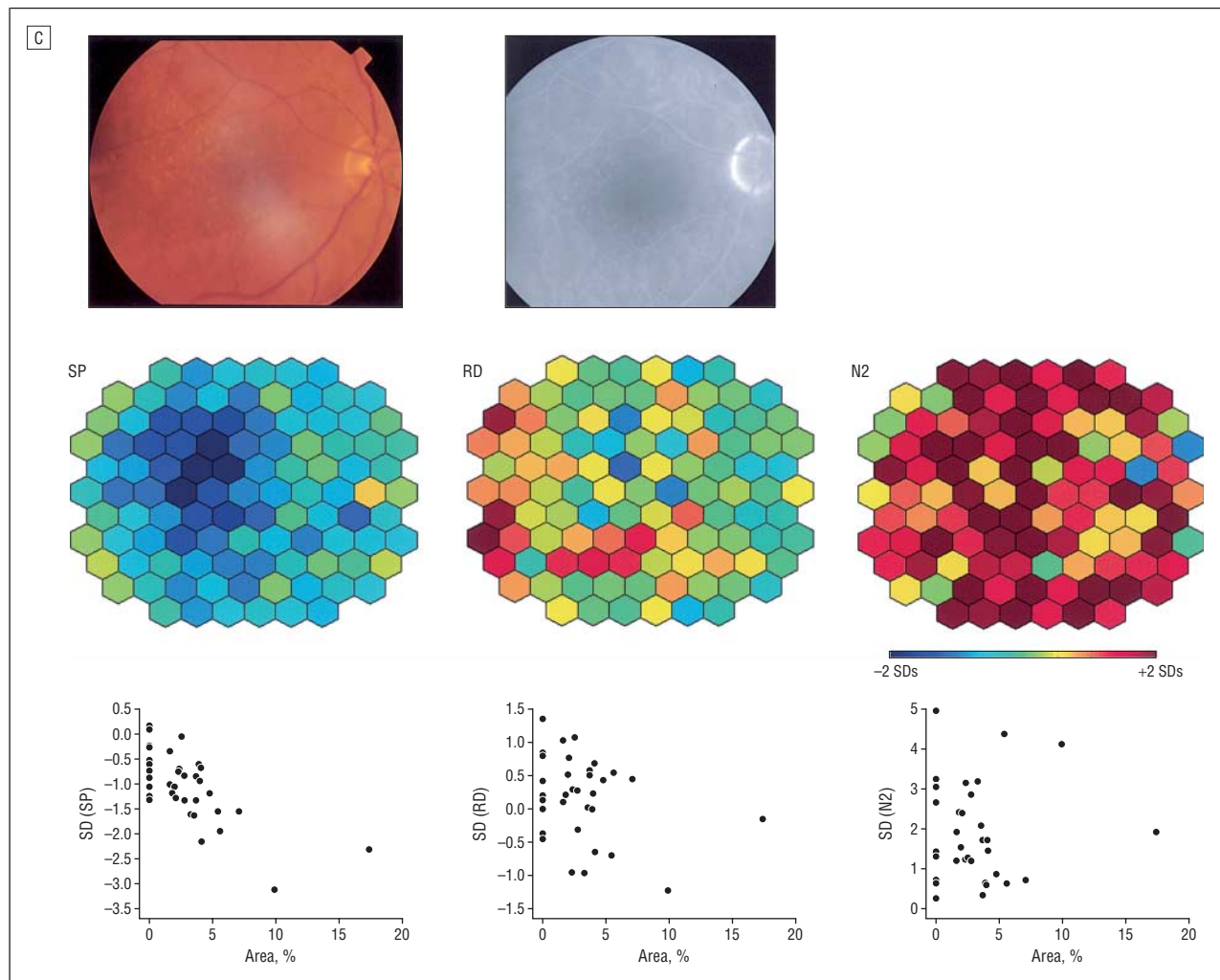


Figure 6C. Correlation of retinal dysfunction and morphologic characteristics for patient 13 (right eye). Color fundus photographs and fluorescein angiograms are shown to illustrate morphologic changes (top row). Multifocal electroretinogram (mfERG) variables are plotted in color-coded units of SD from the control subjects (scalar product [SP], response density P1-N1 [RD], and implicit time N2) (middle row). See the legend to Figure 6A for an explanation of the color coding and scatter diagrams.

nal function. Among the 5 mfERG variables, the scalar product was more often correlated with morphologic changes than the other variables. This finding was not unexpected, since the scalar product reflects changes in both response density and implicit times.¹¹

The percentage of the staining or window defect area in FA was significantly correlated with 3 of 5 mfERG variables in 4 eyes, as shown in **Figure 6**. In each of the examples, color fundus and FA fundus photography are shown in the top row. In the middle row, mfERG responses (scalar product [SP], response density P1-N1 [RD], and implicit time N2 [patients 3, 4, and 13] or P1 [patient 16]) are plotted in terms of differences from the control subjects expressed in SDs (see key for color code). Abnormal scalar products and response densities are coded in dark blue (<2 SDs) and delayed implicit times in red (>2 SDs). In each of the 4 examples, only the mfERG variables that demonstrated a significant correlation with the morphologic changes in FA are shown. The corresponding scatter diagrams are presented in the bottom row. Figure 6A shows the data from a 77-year-old patient with large drusen at the posterior pole. Color-

coded mfERG plots demonstrate a scalar product and response density loss of more than 2 SDs confined over the central areas. Delay in N2 implicit time was found in the central area and also in areas outside a 15° radius. In patient 4 (Figure 6B), scalar product losses are well demarcated in the central 15°, whereas only a few areas show a response density loss greater than 2 SDs. In the same patient, N2 implicit time delays were found in central and peripheral areas tested. In patient 13 (Figure 6C), unlike patient 16 (Figure 6D), there are often reduced scalar products but almost normal response densities (only 1 area with reduced response density >2 SDs in both patients). Implicit time N2 in patient 13 (Figure 6C) was reduced in areas over the entire field tested. In all patients shown in Figure 6 there was a statistically significant correlation between the scalar product or response density loss and implicit time delay (N2 in patients 3, 4, and 13 in Figure 6A-C, P1 in patient 16 in Figure 6D) and the percentage of the staining or window defect area in FA, illustrated in the scatter plots (bottom row).

We asked whether areas without morphologic changes exhibit retinal dysfunction captured by mfERG

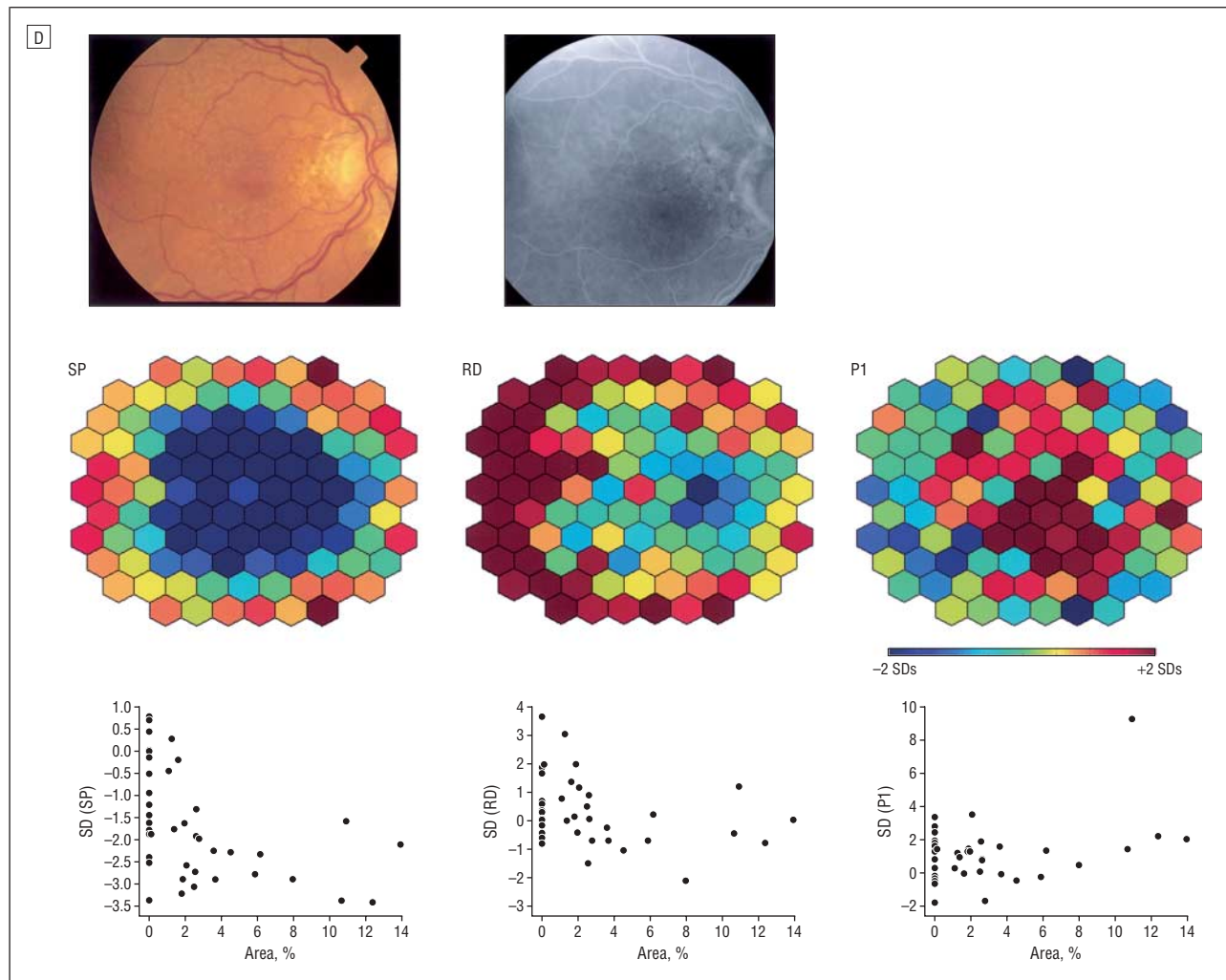


Figure 6D. Correlation of retinal dysfunction and morphologic characteristics for patient 16 (right eye). Color fundus photographs and fluorescein angiograms are shown to illustrate morphologic changes (top row). Multifocal electroretinogram (mfERG) variables are plotted in color-coded units of SD from the control subjects (scalar product [SP], response density P1-N1 [RD], and implicit time P1) (middle row). See the legend to Figure 6A for an explanation of the color coding and scatter diagrams.

responses. To address this question, mfERG data in areas without drusen (RF) or staining or window defect (FA) were analyzed separately. **Figure 7** shows the mfERG variables as units of SD from the control subjects for areas without morphologic changes. For areas without visible morphologic changes in FA, abnormal scalar products and response densities P1-N1 were found for 11.7% and 4.9%, respectively. Significantly delayed implicit times N1, P1, and N2 were found in 12.3%, 19.7%, and 24.3% of the normal retinal areas in FA, respectively. Similar relations were found for areas without visible morphologic changes in RF.

The presence of retinal dysfunction in areas without morphologic changes is illustrated for 3 patients in **Figure 8**. Color fundus photography and mfERG scalar product and implicit time P1 plots (in color-coded units of SD from the control group) are shown. Each of these patients exhibits centrally defined drusen, but in none was there a statistically significant correlation between morphologic features and retinal function. The mfERG responses in patient 3 (left column) showed reduced scalar products mostly in the temporal retinal area

and delayed implicit time P1 in areas over the entire field tested, without any clear relation to areas with drusen. In the middle column (patient 5), there was a more widespread implicit time delay P1 compared with the scalar product loss. In patient 14 (right column), mfERG analysis showed a substantial reduction in scalar product and delays in implicit time P1 extending over the whole test area as demonstrated in the color-coded SD plots.

COMMENT

This study demonstrated that eyes with large drusen exhibit dysfunction in the cone-driven pathways. The abnormal first-order kernel responses point to dysfunctional ON and OFF bipolar and photoreceptor cells as the site of origin.²³ The topographic comparison of the mfERG responses demonstrated a higher sensitivity for implicit time than response density in demonstrating abnormal responses in our cohort. Delayed implicit times reflect an altered synaptic transmission rather than cell loss. It implies that the outer retinal layers in eyes with large drusen exhibit notable functional abnormalities before cell

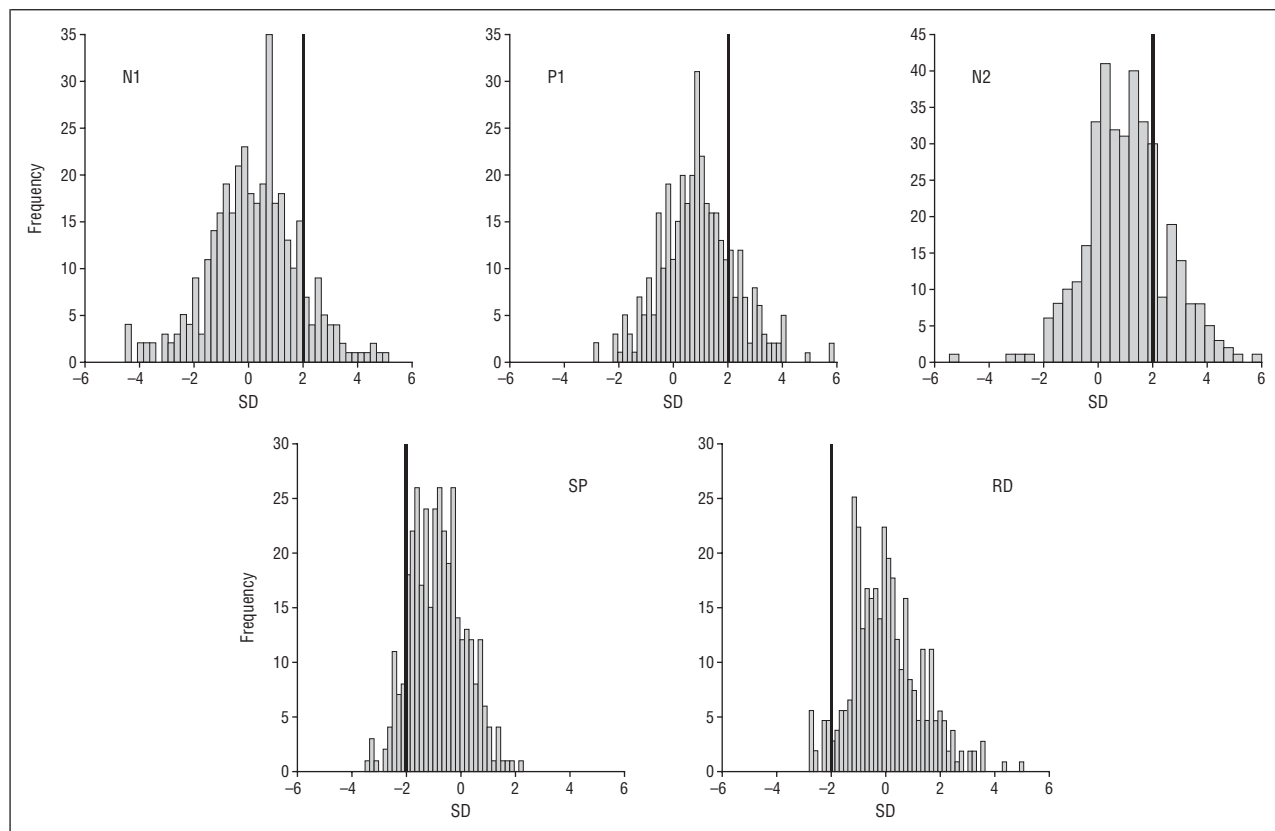


Figure 7. Multifocal electroretinogram responses from areas without morphologic changes (staining or window defect on fluorescein angiograms). Those responses are compared with the healthy control group in histograms for implicit times N1, P1, and N2 and for the scalar product (SP) and response density P1-N1 (RD). Axes are as in Figure 4.

losses. These results agree with those of Takiura et al¹⁵ based on 39 eyes with soft drusen. Concentric ring analysis demonstrated delayed implicit time over the central 30°, and this measure proved to be more sensitive than measures of response density. The topographic analysis by Martinsen¹⁹ in 18 patients with soft drusen larger than 63 μ m showed abnormal response densities (calculated by means of the scalar product method) and P1 implicit times in 26% of the focal responses, whereas response amplitude was abnormal in 10% of the focal responses. The percentage of focal areas with abnormal scalar product and implicit time P1 were higher than in our study (10% and 18.9%, respectively). The difference in cohort size, age, and possibly stage of disease and underlying pathogenetic factors might be responsible for the dissimilar results from our study. In addition, we compared the patient data with data from age-matched controls. Age-matched comparisons provide a more sensitive approach for detecting differences than do comparisons of patient data with one set of averaged data from control subjects. Sandberg et al²⁴ tested patients with drusen who showed neovascular AMD in the contralateral eye and reported significant delayed implicit times, but normal amplitudes in foveal cone ERGs. Similar findings were reported for patients with retinitis pigmentosa. Hood et al²⁵ showed that mfERG response delays are an early indicator of local dysfunction in the cone-driven pathways in retinitis pigmentosa.

Our results suggest that changes in implicit times N1, P1, and N2 are not closely correlated in retinal areas

with large drusen. A delayed implicit time of the first negative component will not necessarily be followed by a delayed P1 or N2 component. Recent studies by Hood et al²³ demonstrated that ON and OFF bipolar cells and photoreceptors contribute and interact differently with the leading and trailing edge of the N1 and P1 components. The time separation of these waveform characteristics in our cohort might imply an inhomogeneous disease impact on outer retinal cells. Implicit time N2 was more often abnormal than implicit times N1 and P1. This suggests an early outer retinal dysfunction in cells other than the photoreceptors.

Using the multifocal recording technique, we were able to detect localized dysfunction in the cone-driven pathways up to 25° in eccentricity. The retinal dysfunction was not restricted to morphologic changes and did not correlate with morphologic findings in most cases. Martinsen¹⁹ performed a similar analysis with morphologic changes defined by discrete categories rather than on a continuous scale using color fundus photography. He found increasing abnormalities in response density and implicit time P1 with increasing drusen area.

Large drusen are also associated with dysfunction in the scotopic pathways. Psychophysical studies of patients with drusen showed abnormal scotopic retinal sensitivity that was not restricted to areas with morphologic change.²⁶ Owsley et al²⁷ reported reduced scotopic sensitivity, exceeding the photopic sensitivity loss in patients with early AMD. No correlation between the amount

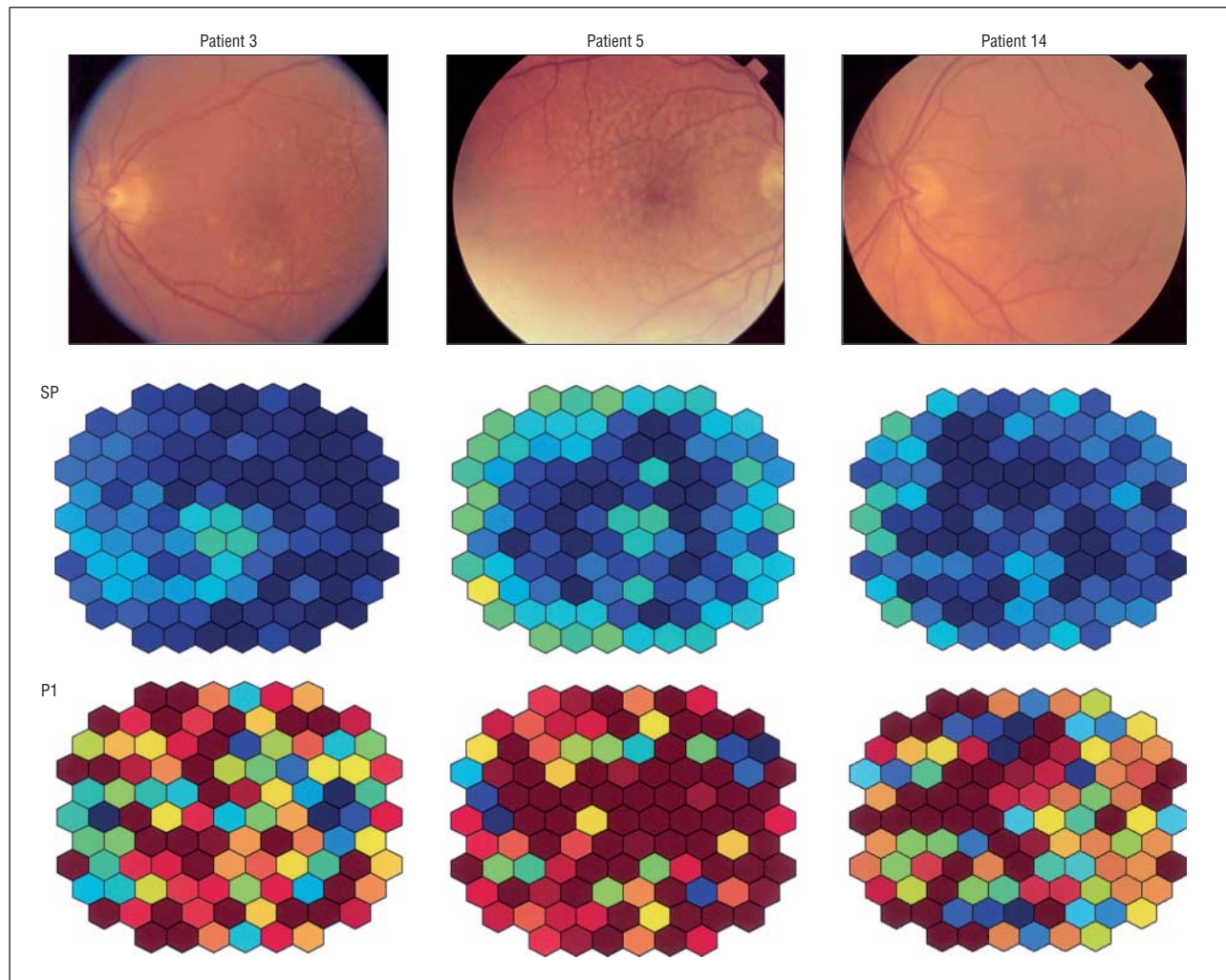


Figure 8. Retinal dysfunction beyond morphologic fundus changes for 3 patients (left column, patient 3 [left eye]; middle column, patient 5 [right eye]; right column, patient 14 [left eye]). Color fundus photographs demonstrate centrally defined drusen (top row). Color-coded units of SD from the control subjects for the scalar product (SP) (middle row) and implicit time P1 (bottom row) illustrate extended retinal dysfunction. Abnormal scalar products are coded in dark blue (<2 SDs) and delayed implicit times of more than 2 SDs in red. Color-coded key is as in Figure 6.

of drusen and dark- or light-adapted sensitivity was found in this study.²⁷ The results of our research, together with the psychophysical findings, point out that large drusen are an early morphologic sign associated with a general dysfunction in the cone- and rod-driven pathways.

In summary, we have assessed a localized dysfunction in the cone-driven pathways in patients with large drusen. Retinal dysfunction extended beyond the drusen and therefore did not correlate with the morphologic changes in most cases. Implicit times are a more sensitive measure than scalar products for detecting retinal dysfunction in those patients.

Submitted for publication December 4, 2002; final revision received May 1, 2003; accepted May 30, 2003.

This study was supported by grant AG04058 from the National Institute on Aging, Bethesda, Md; core grant EY12576 from the National Eye Institute, Bethesda; and a Jules and Doris Stein Research to Prevent Blindness Professorship, Research to Prevent Blindness, New York, NY.

We thank Susan Garcia for help with the patients.

Corresponding author and reprints: Christina Gerth, MD, Department of Ophthalmology, St Franziskus-Hospital, Hohenzollernring 74, 48145 Münster, Germany (e-mail: chgerth@web.de).

REFERENCES

1. Klein R, Klein BE, Jensen SC, Meuer SM. The five-year incidence and progression of age-related maculopathy: the Beaver Dam Eye Study. *Ophthalmology*. 1997;104:7-21.
2. Bressler SB, Maguire MG, Bressler NM, Fine SL. Relationship of drusen and abnormalities of the retinal pigment epithelium to the prognosis of neovascular macular degeneration. *Arch Ophthalmol*. 1990;108:1442-1447.
3. Bird AC, Bressler NM, Bressler SB, et al, the International ARM Epidemiological Study Group. An international classification and grading system for age-related maculopathy and age-related macular degeneration. *Surv Ophthalmol*. 1995;39:367-374.
4. Klein R, Klein BE, Jensen SC. The relation of cardiovascular disease and its risk factors to the five-year incidence of age-related maculopathy: the Beaver Dam Eye Study. *Ophthalmology*. 1997;104:1804-1812.
5. Mitchell P, Wang JJ, Smith W, Leeder SR. Smoking and the 5-year incidence of age-related maculopathy: the Blue Mountains Eye Study. *Arch Ophthalmol*. 2002; 120:1357-1363.

6. Pauleikhoff D, Zuels S, Sheraidah GS, Marshall J, Wessing A, Bird AC. Correlation between biochemical composition and fluorescein binding in Bruch's membrane. *Ophthalmology*. 1992;99:1548-1553.
7. Mullins RF, Johnson LV, Anderson DH, Hageman GS. Characterization of drusen-associated glycoconjugates. *Ophthalmology*. 1998;104:288-298.
8. Sarks SH, Sarks JP. Age-related maculopathy: nonneovascular age-related macular degeneration and the evolution of geographic atrophy. In: Schachat AP, ed. *Retina*. St Louis, Mo: Mosby-Year Book; 2001:1064-1099.
9. Curcio CA, Medeiros NE, Millican CL. Photoreceptor loss in age-related macular degeneration. *Invest Ophthalmol Vis Sci*. 1996;37:1236-1249.
10. Medeiros NE, Curcio CA. Preservation of ganglion cell layer neurons in age-related macular degeneration. *Invest Ophthalmol Vis Sci*. 2001;42:795-803.
11. Sutter EE. The fast m-transform: a fast computation of cross-correlations with binary m-sequences. *SIAM J Comput*. 1991;20:686-694.
12. Sutter EE, Tran D. The field topography of ERG components in man, I: the photopic luminance response. *Vision Res*. 1992;32:433-446.
13. Huang S, Wu D, Jiang F, et al. The multifocal electroretinogram in age-related maculopathies. *Doc Ophthalmol*. 2000;101:115-124.
14. Li J, Tso MO, Lam TT. Reduced amplitude and delayed latency in foveal response of multifocal electroretinogram in early age related macular degeneration. *Br J Ophthalmol*. 2001;85:287-290.
15. Takiura K, Yuzawa M, Miyasaka S. Multifocal electroretinogram in patients with soft drusen in macula [ARVO abstract]. *Invest Ophthalmol Vis Sci*. 2001;42 (suppl):S73.
16. Kretschmann U, Seeliger M, Ruether K, Usui T, Zrenner E. Spatial cone activity in diseases of the posterior pole determined by multifocal electroretinography. *Vision Res*. 1998;38:3817-3828.
17. Palmowski AM, Sutter EE, Bearse MA, Fung W. Multifokales Elektroretinogramm (MF-ERG) in der Diagnostik von Makulaveränderungen. *Ophthalmologe*. 1999;96:166-173.
18. Heinemann-Vernaleken B, Palmowski AM, Allgayer R, Ruprecht KW. Comparison of different high resolution multifocal electroretinogram recordings in patients with age-related maculopathy. *Graefes Arch Clin Exp Ophthalmol*. 2001; 239:556-561.
19. Martinsen GL. *The Multifocal Electroretinogram in Aging and Age-Related Macular Degeneration* [thesis]. Berkeley: University of California; 2000.
20. Gerth C, Garcia SM, Ma M, Keltner JL, Werner JS. Multifocal electroretinogram: age-related changes for different luminance levels. *Graefes Arch Clin Exp Ophthalmol*. 2002;240:202-208.
21. Marmor M, Hood D, Keating D, Kondo M, Seeliger M, Miyake Y. Guidelines for basic multifocal electroretinography (mfERG). Available at: <http://www.iscev.org/standards/index.html>. Accessed October 2001.
22. Werner JS, Gerth C. Optical and neural factors mediating senescent changes in multifocal electroretinogram response. Paper presented at: Annual meeting of the Association for Research in Vision and Ophthalmology; May 6, 2002; Fort Lauderdale, Fla.
23. Hood DC, Frishman LJ, Saszik S, Viswanathan S. Retinal origins of the primate multifocal ERG: implications for the human response. *Invest Ophthalmol Vis Sci*. 2002;43:1673-1685.
24. Sandberg MA, Miller S, Gaudio AR. Foveal cone ERGs in fellow eyes of patients with unilateral neovascular age-related macular degeneration. *Invest Ophthalmol Vis Sci*. 1993;34:3477-3480.
25. Hood DC, Holopigian K, Greenstein V, et al. Assessment of local retinal function in patients with retinitis pigmentosa using the multi-focal ERG technique. *Vision Res*. 1998;38:163-179.
26. Sunness JS, Johnson MA, Massof RW, Marcus S. Retinal sensitivity over drusen and nondrusen areas. *Arch Ophthalmol*. 1988;106:1081-1084.
27. Owsley C, Jackson GR, Cideciyan AV, et al. Psychophysical evidence for rod vulnerability in age-related macular degeneration. *Invest Ophthalmol Vis Sci*. 2000; 41:267-273.

Notice to Authors: Submission of Manuscripts

Selected manuscripts submitted to the *Archives of Ophthalmology* will be submitted for electronic peer review. Please enclose a diskette with your submission containing the following information:

File name
 Make of computer
 Model number
 Operating system
 Word processing program and version number